

NANO EXPRESS

Open Access



Photoconductivities in MoS₂ Nanoflake Photoconductors

Wei-Chu Shen¹, Ruei-San Chen^{2*} and Ying-Sheng Huang¹

Abstract

Photoconductivities in molybdenum disulfide (MoS₂) layered nanostructures with two-hexagonal crystalline structure prepared by mechanical exfoliation were investigated. The photoconductor-type MoS₂ nanoflakes exhibit remarkable photoresponse under the above bandgap excitation wavelength of 532 nm at different optical intensity. The photocurrent responsivity and photoconductive gain of nanoflakes can reach, respectively, 30 AW⁻¹ and 103 at the intensity of 50 Wm⁻², which are several orders of magnitude higher than those of their bulk counterparts. The vacuum-enhanced photocurrent and power-independent responsivity/gain indicate a surface-controlled photoconduction mechanism in the MoS₂ nanomaterial.

Keywords: Molybdenum disulfide, Layer semiconductor, Nanostructure, Photoconductivity, Responsivity, Gain

Background

Molybdenum disulfide (MoS₂), a layer semiconductor with an indirect bandgap of 1.2 eV, has been studied most frequently among the big material family of transition metal dichalcogenide (TMD) [1]. Distinct from their bulk counterparts, recently, MoS₂ monolayers exhibiting direct-bandgap property and enhanced photoluminescence efficiency due to the quantum confinement effect have been discovered [2, 3]. This finding opens up a brand new research direction for TMD layer semiconductors as the building blocks for optoelectronic applications. Integration of MoS₂ and graphene could also realize the full two-dimensional (2D) material heterostructures [4], which is an ideal system for the development of next-generation ultrathin, flexible, and transparent light-emitting [5], light-harvesting [6, 7], and light-detecting devices [8, 9].

Taking the advantages of 2D structure and high quantum efficiency [7], the MoS₂ monolayers and multilayers prepared by mechanical exfoliation and coating techniques have been demonstrated to be an active material for light-detecting devices [10–16]. Among them, most reports investigated the photodetectors based on the configuration of field-effect transistor (FET). The 2D MoS₂ phototransistors exhibit ultrahigh responsivity and rapid response to the

light in the visible range. However, fundamental photoconduction (PC) properties in the pristine MoS₂ and its nanostructures were rarely investigated. Here, we report on a comparative study of the photoconductor-type MoS₂ nanoflakes and their bulk counterparts. The photoconduction performance was investigated by quantitatively defining responsivity and photoconductive gain. The mechanism was also discussed by the light intensity- and environment-dependent PC measurements.

Methods

The MoS₂ layer crystals used for this study were grown using the chemical vapor transport (CVT) method using bromine (Br) as the transport agent [17]. The source material powders including molybdenum and sulfur together with the bromine were sealed in a quartz ampoule at a vacuum degree of 2×10^{-5} Torr. Prior to the CVT growth process, the ampoules were annealed at 1050 °C in an oven for 1 month to compound the source materials. The temperatures of the source and crystallization ends were, respectively, controlled at 1050 and 960 °C during the CVT growth. The MoS₂ nanoflakes were obtained by exfoliating bulk crystals using dicing tape and were then dispersed on the insulating SiO₂ (300 nm)/*n*-Si templates with pre-patterned Ti/Au circuits. Two platinum (Pt) metal contacts were subsequently deposited on the selected MoS₂ flakes using focused-ion beam (FIB) technique. The voltage and current of the ion beam for

* Correspondence: rsc@mail.ntust.edu.tw

²Graduate Institute of Applied Science and Technology, National Taiwan University of Science and Technology, Taipei 10607, Taiwan
Full list of author information is available at the end of the article

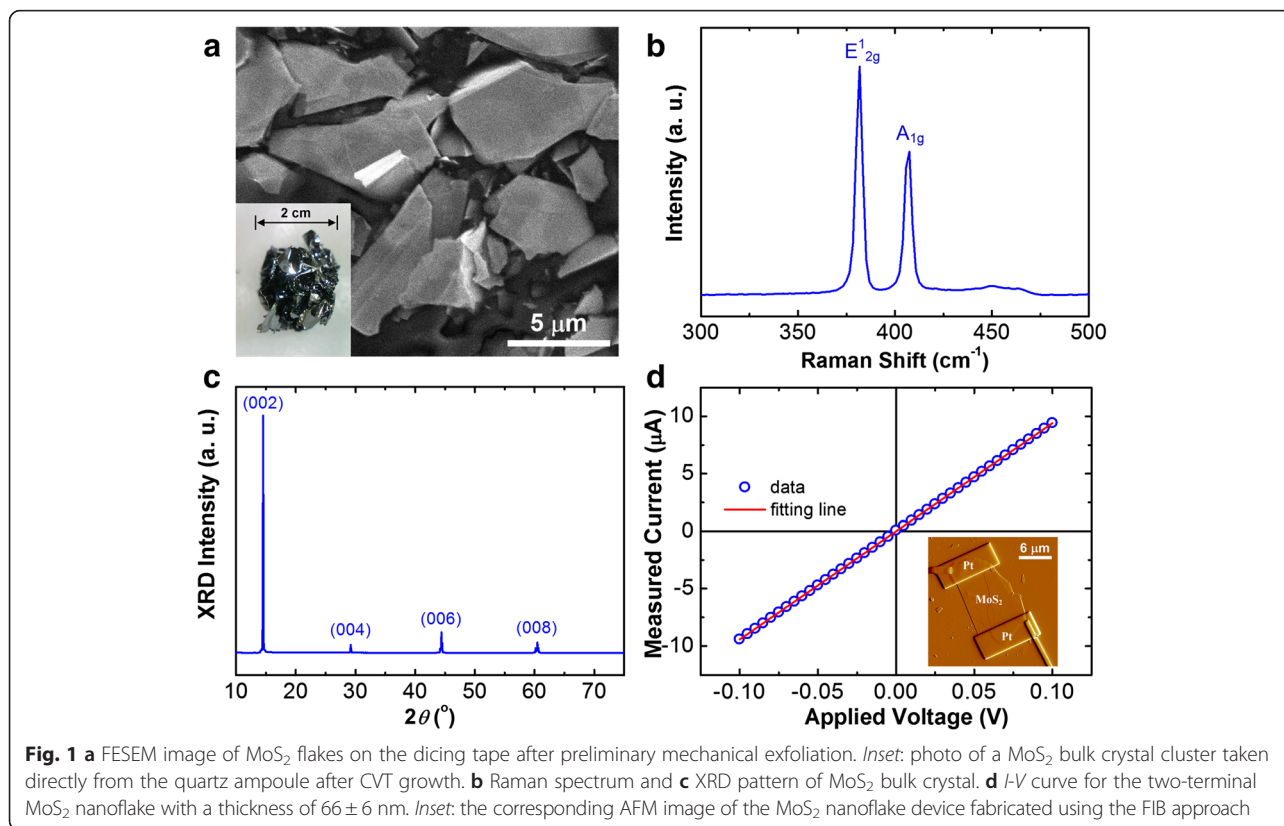
the Pt precursor decomposition were operated at 30 kV and 100 pA, respectively. In addition, silver paste was used for the metal electrode of the millimeter-sized MoS₂ bulks. The crystal quality of MoS₂ was characterized using field-emission scanning electron microscopy (FESEM), Raman spectroscopy, and X-ray diffractometry (XRD). The thicknesses of the MoS₂ flakes were defined by the atomic force microscopy (AFM). Electrical characterization was performed at an ultralow current leakage probe station (Lake-Shore Cryotronics TTP4). The dc voltage and current were, respectively, sourced and measured by a semiconductor characterization system (Keithley 4200-SCS). A Nd:YAG laser with a wavelength of 532 nm was used as an excitation light source for the photoconductivity measurement. An optical diffuser was used to broaden laser beam size (~20 mm²) to uniformly illuminate the conduction channel of the nanoflake and bulk samples for the steady-state photocurrent measurements. The incident laser power was measured by a calibrated power meter (Ophir Nova II) with a silicon photodiode head (Ophir PD300-UV).

Results and Discussion

Figure 1a depicts a FESEM image of the MoS₂ flakes after preliminary mechanical exfoliation. The flakes on the dicing tape show irregular shapes, and their area sizes were reduced to micrometer scale from the millimeter-sized bulk

crystals. A photo in the inset of Fig. 1a shows a cluster of MoS₂ single crystals taken directly from the quartz ampoule after CVT growth. Figure 1b depicts a Raman spectrum of a MoS₂ single crystal using the light source of 414.5 nm wavelength. Two major peaks were observed, and their peak positions determined by curve fitting are at 382 and 407 cm⁻¹, which are, respectively, consistent with the E_{2g}¹ and A_{1g} modes for the 2H-MoS₂ [18]. The full width at half maximum (FWHM) values of the Raman peaks are 2.7 (E_{2g}¹) and 3.7 (A_{1g}) cm⁻¹. The XRD measurement was also used to characterize the structural quality of the MoS₂ layer crystals. Figure 1c depicts an XRD pattern with four diffraction peaks centered at 14.5°, 29.2°, 44.4°, and 60.4°. These peaks are indexed as (002), (004), (006), and (008) diffraction planes, respectively, according to the database (JCPDS #872416). The single one out-of-plane orientation of ⟨001⟩ (*c*-axis) further confirms the crystalline quality of the 2H-MoS₂.

In addition, the electric contacts of MoS₂ nanoflake devices were examined by the two-terminal current versus voltage (*I*-*V*) measurement. Figure 1d depicts a representative *I*-*V* curve for the MoS₂ nanoflake with a thickness of 66 ± 6 nm. The linear *I*-*V* relationship indicates a good ohmic contact condition of the photoconductor-type device. The details of ohmic contact fabrication using FIB technique for the TMD layered nanostructures can be



found in our earlier publications [19, 20]. The corresponding AFM image of the nanoflake device is also shown in the insets of Fig. 1d.

Photocurrent responses under the excitation of 532 nm wavelength (λ) at a bias of 0.1 V and at different laser powers for a MoS₂ nanoflake ($t = 45$ nm) were shown in Fig. 2a. For comparison, the photoresponse measurement under the same excitation condition at a bias of 1 V for a bulk crystal ($t = 63$ μm) was also performed and is shown in Fig. 2b. All the background dark currents were subtracted from the response curves to reveal the photocurrent values. The results show that both the nanoflake and the bulk exhibit clear photoresponse to the different excitation power and the photocurrent increases with an increase of power.

The difference in photocurrent level between the nanoflake and bulk can be observed by the plot of photocurrent (i_p) versus intensity (I), Fig. 3a. From the result, it is noticed that the overall photocurrent of the bulk is approximately one to two orders of magnitude higher than that of the nanostructure. In addition, the photocurrent value is linearly dependent on the intensity,

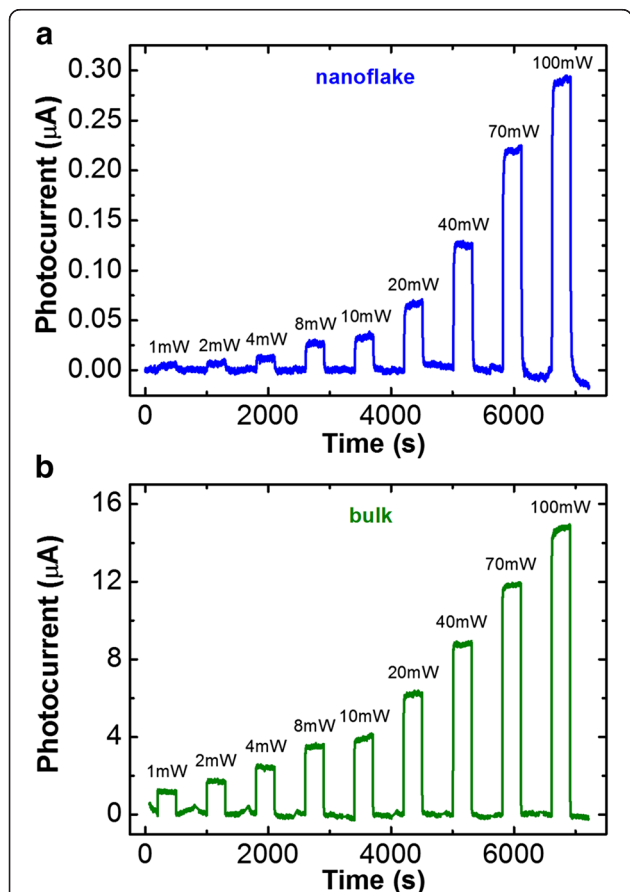


Fig. 2 a Photocurrent responses to the different light power and the excitation wavelengths of 532 nm measured in air ambience for a the MoS₂ nanoflake ($t = 45$ nm) and b the bulk crystal ($t = 63$ μm)

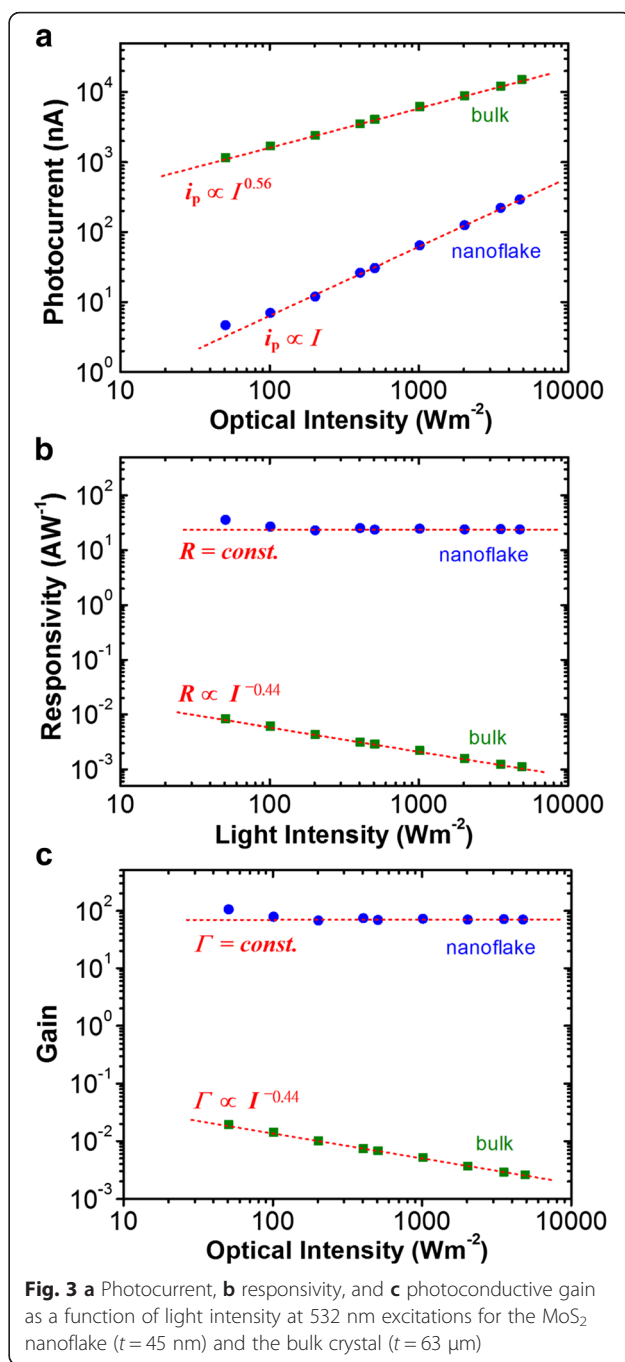


Fig. 3 a Photocurrent, b responsivity, and c photoconductive gain as a function of light intensity at 532 nm excitations for the MoS₂ nanoflake ($t = 45$ nm) and the bulk crystal ($t = 63$ μm)

i.e., $i_p \propto I$, for the nanoflake. The intensity-dependent behavior is different from the bulk. The photocurrent is less sensitive to the increase in light intensity, and their relationship follows a power law of $i_p \propto I^\beta$, where $\beta = 0.56$, for the bulk.

Photoconduction is a two-step process that consists of light absorption and carrier collection. Photocurrent value depends on the extrinsic properties of device such as applied bias and electrode inter-distance and the intrinsic properties of material such as carrier mobility

and lifetime. To understand the performance of the MoS₂ photoconductors and their underneath mechanism, two critical parameters including photocurrent responsivity and photoconductive gain were investigated.

The responsivity (R) value is a measure of photocurrent generation efficiency of a photodetector and is defined as the photocurrent generated by the power of light incident on an effective area of a photoconductor (P). Therefore, responsivity is written as

$$R = \frac{i_p}{P}, \quad (1)$$

where $P = IA = Iwl$, where A is the projected area of the photoconductor ($A = wl$), w is the width, and l is the length of the photoconductor [21]. Figure 3b depicts the calculated responsivity as a function of light intensity. The result shows that the responsivity value does not exhibit a definable change with an increase in excitation intensity for the MoS₂ nanoflake. The responsivity varies at a small range of 20–30 AW⁻¹. The values of the MoS₂ nanoflake are over three orders of magnitude higher than those ($R = 0.001 - 0.009$ AW⁻¹) of the bulk in the intensity range of 50–5000 Wm⁻².

The MoS₂ flake device belongs to a two-terminal photoconductor-type photodetector without applied gate bias. Compared to the other 2D material photoconductors, the responsivity values of the MoS₂ nanoflake are much higher than those of the reduced graphene oxide ($R = 0.004$ AW⁻¹) [22], graphene nanoribbon ($R = 1$ AW⁻¹) [22], and MoS₂ multilayer films ($R = 0.071 - 1.8$ AW⁻¹) [10–12] and are comparable with the GaS ($R = 4.2 - 19.2$ AW⁻¹) [23] and GaSe ($R \sim 2.8$ AW⁻¹) [24] nanosheets. On the other hand, three-terminal phototransistors of 2D materials usually exhibit better detector performance due to the field effect. However, if compared to these phototransistors, the responsivity values of the MoS₂ nanoflake are still higher than those of the graphene ($R = 0.0005 - 0.0061$ AW⁻¹) [25, 26] and partial MoS₂ monolayer ($R = 0.0075 - 6$ AW⁻¹) [13, 14] phototransistors but are lower than the optimally reported values of the MoS₂ monolayer ($R = 880$ AW⁻¹) [15], surface-modified MoS₂ and WSe₂ ($R = 5750 - 14,500$ AW⁻¹) [16], graphene/quantum dots ($R \sim 10^7$ AW⁻¹) [27] and MoS₂/graphene ($R = 1.6 \times 10^4 - 5 \times 10^8$ AW⁻¹) [8, 9, 28] hybrid phototransistors.

It is interesting that the nanostructure has lower photocurrent but exhibits higher photocurrent generation efficiency (i.e., responsivity) compared to the bulk. According to the definition of responsivity, the measured photocurrent is divided by the projected area. Though photocurrent of the bulk is two orders of magnitude higher than that of the nanoflake, the projected area of the bulk crystal ($A = 1.1 \times 2.5$ mm²) is six orders of magnitude larger than that of the nanoflake ($A = 1.2 \times 2.2$ μm²). The analysis mathematically explains that the

nanoflake device produces less photocurrent but exhibits higher generation efficiency. However, to further understand the physical origins of the superior photodetector performance in the MoS₂ 2D structures, photoconductive gain was investigated.

Gain (Γ) value conceptually means the circulating number of carrier transport through a photoconductor per unit time before recombination. Therefore, gain is defined as the ratio of carrier lifetime (τ) to transit time (τ_t) between two electrodes and is written as

$$\Gamma = \frac{\tau}{\tau_t} = \frac{V}{l^2} \tau \mu, \quad (2)$$

where μ is the mobility [21, 29]. Because gain has a linear relationship with responsivity and photocurrent, the gain value can be estimated according to the equation

$$\Gamma = \frac{ER}{e\eta} = \frac{E}{e} \frac{i_p}{\eta P}, \quad (3)$$

where E is the photon energy, e is the elementary charge, and η is the quantum efficiency [29].

To simplifying the calculation, the reflection loss was neglected and thus the quantum efficiency can be expressed as $\eta = 1 - e^{-\alpha t}$, where α is the optical absorption coefficient and t is the sample thickness. According to the literatures, the α value of the MoS₂ is approximately 3.5×10^5 cm⁻¹ for the absorption wavelength near 532 nm (2.33 eV) [30]. The calculated η values are 79 and 100 % for the nanoflake ($t = 45$ nm) and the bulk ($t = 63$ μm), respectively.

The calculated gain as a function of intensity is shown in Fig. 3c. The result indicates the gain values ($\Gamma = 66 - 103$) of the nanoflake is over three orders of magnitude higher than those ($\Gamma = 0.0026 - 0.019$) of the bulk. In addition, the gain values have been investigated rarely for the photoconductor-type 2D materials compared to other nanomaterial systems, but these values are higher than those of ZnS nanobelts ($\Gamma \sim 0.5$) [31], ZnSe nanobelts ($\Gamma \sim 0.4$) [32], ZnO nanospheres ($\Gamma \sim 5$) [33], and Nb₂O₅ nanobelts ($\Gamma \sim 6$) [34] and are lower than the optimal reported values for the ZnO nanowire ($\Gamma \sim 2 \times 10^8$) [35], SnO₂ nanowire ($\Gamma \sim 8 \times 10^8$) [36], GaN nanowire ($\Gamma \sim 10^8$) [37] photoconductors, graphene/quantum dot ($\Gamma \sim 10^8$) [27], and MoS₂/graphene ($\Gamma = 10^7 - 4 \times 10^{10}$ AW⁻¹) [8, 9, 28] hybrid phototransistors.

Photoconductive gain has a physical meaning of the excess carrier collection efficiency in a photodetector. According to Eq. (2), gain value depends on electrode interspace and applied bias. In this study, the ratio of $\frac{V}{l^2}$ of the nanoflake ($l = 1.2$ μm, $V = 0.1$ V) to the bulk ($l = 1.1$ mm, $V = 1$ V) is approximately 84,000:1. The much higher $\frac{V}{l^2}$ value provides a much shorter transport time

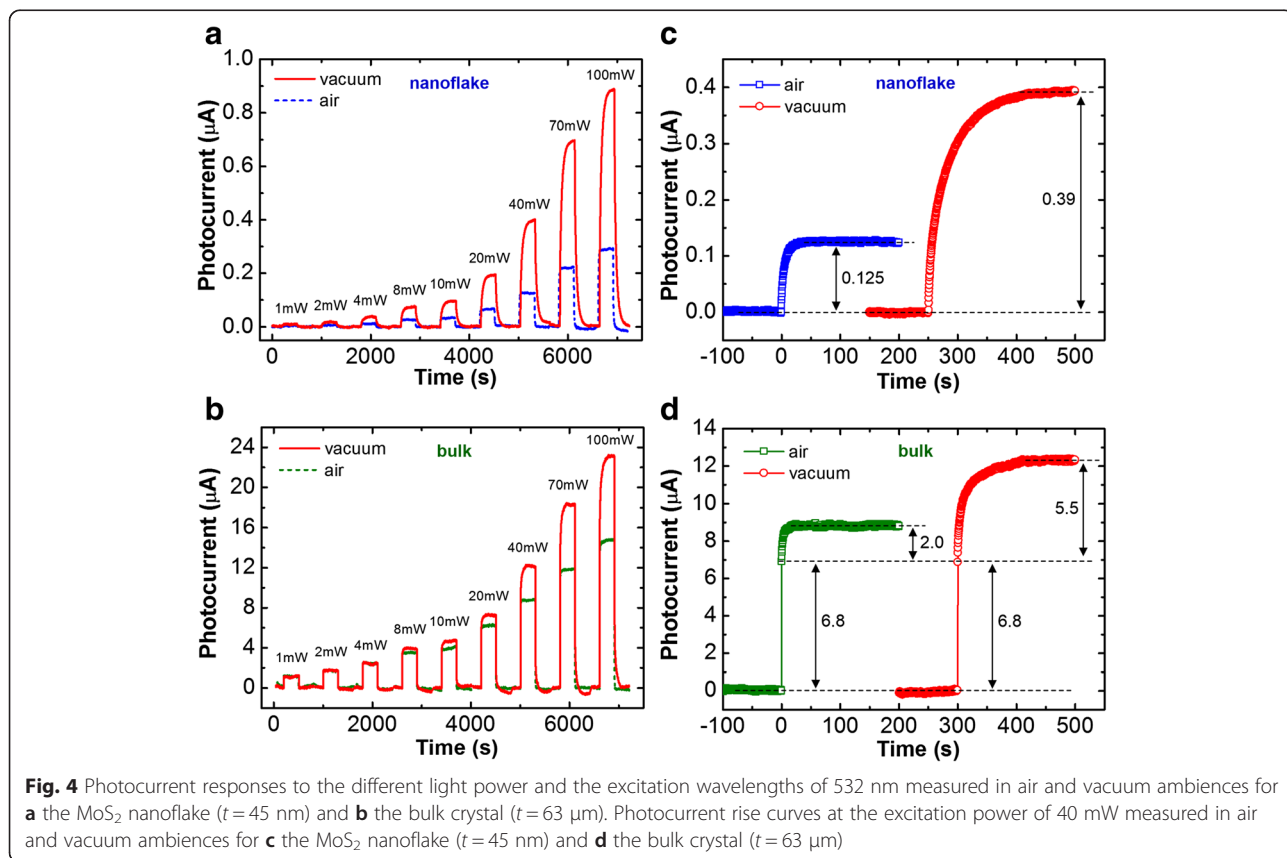
of carrier $\left(\tau_t = \left(\frac{V}{l^2}\mu\right)^{-1}\right)$ and a higher probability of carrier collection, which is the dominant factor for high-gain transport in the MoS₂ nanoflakes.

In addition to the artificial factors of l and V , gain value could also depend on the $\tau\mu$ product which is an intrinsic quantity of a photoconductor. Figure 4a, b illustrates the power-dependent photoresponse curves at the excitation of $\lambda = 532$ nm measured in atmospheric and vacuum ambiances for the MoS₂ nanoflake ($t = 45$ nm, $V = 0.1$ V) and the bulk crystal ($t = 63$ μm , $V = 1$ V). The result shows that the photocurrent of the nanoflake can be remarkably enhanced by changing the ambience from air to vacuum. The enhancement of photocurrent in the bulk is relatively less. The ambience-dependent behavior implies a surface-controlled photoconductivity and is similar to the oxygen-sensitized photoconduction (OSPC) mechanism which has been frequently observed in the metal oxide semiconductors [35, 38].

According to the model, carrier lifetime is determined by oxygen (and water molecule) [39, 40] adsorption rate on the material surface. The carrier lifetime can be prolonged in vacuum because of the lower recombination rate induced by the lower oxygen adsorption rate. The prolonged lifetime increases the photocurrent in vacuum.

Because the bulk crystal has smaller surface-to-volume ratio, the photocurrent can be generated by both core (ambience-independent) and surface (ambience-sensitive) regions. This statement explains the MoS₂ bulk with less enhancement of photocurrent in vacuum.

The aforementioned statement can be further supported by the time-resolved photoresponse measurement. Figure 4c, d depicts the photocurrent rise curves at the excitation power of 40 mW measured in air and vacuum ambiances for the nanoflake and bulk. From Fig. 4d, we can notice that the bulk exhibits a two-stage current rise behavior either in air or in vacuum. A slow current rise (with a photocurrent of 2.0 μA and a rise time of 2.7 s) superposes a relatively fast current response (with a photocurrent of 6.8 μA and a rise time less than 0.3 s) in air. The photocurrent and rise time can be both enhanced to 5.5 μA and 16 s, respectively, when changing the ambience to vacuum. However, the photocurrent section of fast response remains constant and is independent on the environment. The result implies that the fast photoresponse originates from the core bulk region, which is different from the slower one. The slow and environment-sensitive properties are consistent with the description of the OSPC mechanism. The ratio of the OSPC photocurrent in air to that in vacuum is approximately 1:3 for the MoS₂ bulk.



The current enhancement ratio is also consistent with that of the nanoflake shown in Fig. 4c. The fast photoresponse was not observed in the MoS₂ nanoflake, indicating a single surface-dominant photoconduction property.

According to the OSPC mechanism, excess electron lifetime should remain constant because the recombination rate is determined by the oxygen adsorption rate. The constant lifetime is somewhat similar to the hole-trapping mechanism before the trap states are filled [41, 42]. This statement can explain that the responsivity or gain value is independent on the excitation intensity (i.e., R or $I \propto \tau = \text{const.}$) and the photocurrent is linearly proportional to the intensity (i.e., $i_p \propto I$) as observed in Fig. 3. In addition, the bulk exhibits different intensity dependences of photocurrent and responsivity or gain ($i_p \propto I^\beta$, and R or $I \propto I^{\beta-1}$, where $\beta = 0.56$). The power law dependence is consistent with the bimolecular recombination mechanism in the intrinsic semiconductor in which the β value is 0.5 theoretically [41, 43]. The β value of the bulk slightly higher than the theoretical one is probably due to the partial contribution of surface PC mechanism.

Conclusions

Photoconduction performances and mechanisms in the photoconductor-type MoS₂ nanostructures and bulks were investigated and compared. The responsivity and gain values of the MoS₂ nanoflakes are higher than those of the bulk counterparts for several orders of magnitude. An environment-sensitive photoresponse behavior implies the surface-dominant OSPC mechanism in MoS₂ 2D structures. Further investigations on the intrinsic photoconduction properties such as normalized gain [44] and mobility in the pristine MoS₂ nanoflakes are still required and will be elaborated elsewhere.

Competing interests

The authors declare that they have no competing interests.

Authors' contributions

WCS carried out material characterization, device fabrication, and photoconductivity measurements. RSC designed the experiments, analyzed the data, and drafted the manuscript. YSH carried out bulk crystal growth. All authors read and approved the final manuscript.

Acknowledgements

RSC thanks the support of the Ministry of Science and Technology (MOST) of Taiwan under the projects NSC 102-2112-M-011-001-MY3 and MOST 104-2923-M-011-001-MY3.

Author details

¹Department of Electronic Engineering, National Taiwan University of Science and Technology, Taipei 10607, Taiwan. ²Graduate Institute of Applied Science and Technology, National Taiwan University of Science and Technology, Taipei 10607, Taiwan.

Received: 21 January 2016 Accepted: 7 February 2016

Published online: 02 March 2016

References

- Wang QH, Kalantar-Zadeh K, Kis A, Coleman JN, Strano MS (2012) Electronics and optoelectronics of two-dimensional transition metal dichalcogenides. *Nat Nanotech* 7:699
- Mak KF, Lee C, Hone J, Shan J, Heinz TF (2010) Atomically thin MoS₂: a new direct-gap semiconductor. *Phys Rev Lett* 105:136805
- Splendiani A, Sun L, Zhang YB, Li TS, Kim J, Chim CY, Galli G, Wang F (2010) Emerging photoluminescence in monolayer MoS₂. *Nano Lett* 10:1271
- Geim AK, Grigorieva IV (2013) Van der Waals heterostructures. *Nature* 499:419
- Withers F, Del Pozo-Zamudio O, Mishchenko A, Rooney AP, Gholinia A, Watanabe K, Taniguchi T, Haigh SJ, Geim AK, Tartakovskii AI, Novoselov KS (2015) Light-emitting diodes by band-structure engineering in van der Waals heterostructures. *Nat Mater* 14:301
- Britnell L, Ribeiro RM, Eckmann A, Jalil R, Belle BD, Mishchenko A, Kim YJ, Gorbachev RV, Georgiou T, Morozov SV, Grigorenko AN, Geim AK, Casiraghi C, Castro Neto AH, Novoselov KS (2013) Strong light-matter interactions in heterostructures of atomically thin films. *Science* 340:1311
- Bernardi M, Palumbo M, Grossman JC (2013) Extraordinary sunlight absorption and one nanometer thick photovoltaics using two-dimensional monolayer materials. *Nano Lett* 13:3664
- Roy K, Padmanabhan M, Goswami S, Sai TP, Ramalingam G, Raghavan S, Ghosh A (2013) Graphene-MoS₂ hybrid structures for multifunctional photoresponsive memory devices. *Nat Nanotech* 8:826
- Zhang WJ, Chuu CP, Huang JK, Chen CH, Tsai ML, Chang YH, Liang CT, Chen YZ, Chueh YL, He JH, Chou MY, Li LJ (2014) Ultrahigh-gain photodetectors based on atomically thin graphene-MoS₂ heterostructures. *Sci Rep* 4:3826
- Cho B, Kim AR, Park Y, Yoon J, Lee YJ, Lee S, Yoo TJ, Kang CG, Lee BH, Ko HC, Kim DH, Hahn MG (2015) Bifunctional sensing characteristics of chemical vapor deposition synthesized atomic-layered MoS₂. *ACS Appl Mater Interfaces* 7:2952
- Lu JP, Lu JH, Liu HW, Liu B, Chan KX, Lin JD, Chen W, Loh KP, Sow CH (2014) Improved photoelectrical properties of MoS₂ films after laser micromachining. *ACS Nano* 8:6334
- Ling ZP, Yang R, Chai JW, Wang SJ, Leong WS, Tong Y, Lei D, Zhou Q, Gong X, Chi DZ, Ang KW (2015) Large-scale two-dimensional MoS₂ photodetectors by magnetron sputtering. *Opt Express* 23:13580
- Yin ZY, Li H, Jiang L, Shi YM, Sun YH, Lu G, Zhang Q, Chen XD, Zhang H (2012) Single-layer MoS₂ phototransistors. *ACS Nano* 6:74
- Furchi MM, Polyushkin DK, Pospischil A, Mueller T (2014) Mechanisms of photoconductivity in atomically thin MoS₂. *Nano Lett* 14:6165
- Lopez-Sanchez O, Lembke D, Kayci M, Radenovic A, Kis A (2013) Ultrasensitive photodetectors based on monolayer MoS₂. *Nat Nanotech* 8:497
- Kang DH, Kim MS, Shim J, Jeon J, Park HY, Jung WS, Yu HY, Pang CH, Lee S, Park JH (2015) High-performance transition metal dichalcogenide photodetectors enhanced by self-assembled monolayer doping. *Adv Funct Mater* 25:4219
- Tiong KK, Liao PC, Ho CH, Huang YS (1999) Growth and characterization of rhenium-doped MoS₂ single crystals. *J Cryst Growth* 205:543
- Li H, Zhang Q, Yap CCR, Tay BK, Edwin THT, Olivier A, Baillargeat D (2012) From bulk to monolayer MoS₂: Evolution of Raman scattering. *Adv Funct Mater* 22:1385
- Chen RS, Tang CC, Shen WC, Huang YS (2015) Ohmic contact fabrication using a focused-ion beam technique and electrical characterization for layer semiconductor nanostructures. *J Vis Exp*. Article no. e53200, doi:10.3791/53200.
- Chen RS, Tang CC, Shen WC, Huang YS (2014) Thickness-dependent electrical conductivities and ohmic contacts in transition metal dichalcogenides multilayers. *Nanotechnology* 25:415706
- Bhattacharya P (1997) Semiconductor optoelectronic devices. Prentice-Hall Inc., New Jersey, Ch. 8, p 346-351
- Chitara B, Panchakarla LS, Krupanidhi SB, Rao CNR (2011) Infrared photodetectors based on reduced graphene oxide and graphene nanoribbons. *Adv Mater* 23:5419
- Hu PA, Wang LF, Yoon M, Zhang J, Feng W, Wang XN, Wen ZZ, Idrobo JC, Miyamoto Y, Gehegan DB, Xiao K (2013) Highly responsive ultrathin GaS nanosheet photodetectors on rigid and flexible substrates. *Nano Lett* 13:1649
- Hu PA, Wen ZZ, Wang LF, Tan PH, Xiao K (2012) Synthesis of few-layer GaSe nanosheets for high performance photodetectors. *ACS Nano* 6:5988
- Xia FN, Mueller T, Lin YM, Valdes-Garcia A, Avouris P (2009) Ultrafast graphene photodetector. *Nat Nanotech* 4:839

26. Mueller T, Xia FNA, Avouris P (2010) Graphene photodetectors for high-speed optical communications. *Nat Photonics* 4:297
27. Konstantatos G, Badioli M, Gaudreau L, Osmond J, Bernechea M, de Arquer FPG, Koppens FHL (2012) Hybrid graphene-quantum dot phototransistors with ultrahigh gain. *Nat Nanotechnol* 7:363
28. Chen CY, Qiao H, Lin SH, Luk CM, Liu Y, Xu ZQ, Song JC, Xue YZ, Li DL, Yuan J, Yu WZ, Pan CX, Lau SP, Bao QL (2015) Highly responsive MoS₂ photodetectors enhanced by graphene quantum dots. *Sci Rep* 5:11830
29. Razeghi M, Rogalski A (1996) Semiconductor ultraviolet detectors. *J Appl Phys* 79:7433
30. Beal AR, Hughes HP (1979) Kramers-Kronig analysis of the reflectivity spectra of 2H-MoS₂, 2H-MoSe₂ and 2H-MoTe₂. *J Phys C Solid State Phys* 12:881
31. Fang XS, Bando Y, Liao MY, Gautam UK, Zhi CY, Dierre B, Liu BD, Zhai TY, Sekiguchi T, Koide Y, Golberg D, Koide D, Golberg (2009) Single-crystalline ZnS nanobelts as ultraviolet-light sensors. *Adv Mater* 21:2034
32. Fang XS, Xiong SL, Zhai TY, Bando Y, Liao MY, Gautam UK, Koide Y, Zhang X, Qian YT, Golberg D (2009) High-performance blue/ultraviolet-light-sensitive ZnSe-nanobelt photodetectors. *Adv Mater* 21:5016
33. Chen M, Hu LF, Xu JX, Liao MY, Wu LM, Fang XS (2011) ZnO hollow-sphere nanofilm-based high-performance and low-cost photodetector. *Small* 7:2449
34. Fang XS, Hu LF, Huo KF, Gao B, Zhao LJ, Liao MY, Chu PK, Bando Y, Golberg D (2011) New ultraviolet photodetector based on individual Nb₂O₅ nanobelts. *Adv Funct Mater* 21:3907
35. Soci C, Zhang A, Xiang B, Dayeh SA, Aplin DPR, Park J, Bao XY, Lo YH, Wang D (2007) ZnO nanowire UV photodetectors with high internal gain. *Nano Lett* 7:1003
36. Chen RS, Wang WC, Chan CH, Lu ML, Chen YF, Lin HC, Chen KH, Chen LC (2013) Photoconduction efficiencies of metal oxide semiconductor nanowires: The material's inherent properties. *Appl Phys Lett* 103:223107
37. Gonzalez-Posada F, Songmuang R, Den Hertog M, Monroy E (2012) Room-temperature photodetection dynamics of single GaN nanowires. *Nano Lett* 12:172
38. Chen RS, Chen CA, Tsai HY, Wang WC, Huang YS (2012) Photoconduction properties in single-crystalline titanium dioxide nanorods with ultrahigh normalized gain. *J Phys Chem C* 116:4267
39. Chakrapani V, Angus JC, Anderson AB, Wolter SD, Stoner BR, Sumanasekera GU (2007) Charge transfer equilibria between diamond and an aqueous oxygen electrochemical redox couple. *Science* 318:1424
40. Chakrapani V, Pendyala C, Kash K, Anderson AB, Sunkara MK, Angus JC (2008) Electrochemical pinning of the Fermi level: mediation of photoluminescence from gallium nitride and zinc oxide. *J Am Chem Soc* 130:12944
41. Stevens KS, Kinniburgh M, Beresford R (1995) Photoconductive ultraviolet sensor using Mg-doped GaN on Si(111). *Appl Phys Lett* 66:3518
42. Binet F, Duboz JY, Rosencher E, Scholz F, Harle V (1996) Mechanisms of recombination in GaN photodetectors. *Appl Phys Lett* 69:1202
43. Bube RH (1992) Photoelectronic properties of semiconductors. Cambridge University Press, Cambridge. Chap. 2, p 28-30
44. Prades JD, Jimenez-Diaz R, Hernandez-Ramirez F, Fernandez-Romero L, Andreu T, Cirera A, Romano-Rodriguez A, Cornet A, Morante JR, Barth S, Mathur S (2008) Toward a systematic understanding of photodetectors based on individual metal oxide nanowires. *J Phys Chem C* 112:14639

Submit your manuscript to a SpringerOpen[®] journal and benefit from:

- Convenient online submission
- Rigorous peer review
- Immediate publication on acceptance
- Open access: articles freely available online
- High visibility within the field
- Retaining the copyright to your article

Submit your next manuscript at ► springeropen.com
